IEEE Access
Multidisciplinary ⋮ Rapid Review ⋮ Open Access Journal

Received 20 June 2022, accepted 14 July 2022, date of publication 25 July 2022, date of current version 1 August 2022.

Digital Object Identifier 10.1109/ACCESS.2022.3193772

RESEARCH ARTICLE

Data-Driven Analysis for Calculated Time Over in Air Traffic Flow Management

DAICHI TORATANI, YOICHI NAKAMURA, AND MEGUMI OKA
Air Traffic Management Department, Electronic Navigation Research Institute (ENRI), National Institute of Maritime, Port and Aviation Technology (MPAT), Chofu, Tokyo 182-0012, Japan

Corresponding author: Daichi Toratani (toratani-d@mpat.go.jp)

ABSTRACT Excessive air traffic demand saturates air traffic control and causes traffic delays due to limited airspace and airport capacity. Air traffic flow management (ATFM) is used to regulate such demand using traffic management initiatives (TMIs), such as ground delay, miles-in-trail and speed adjustment. The Calculated Time Over (CTO), which is a time-assignment TMI for an in-flight aircraft, is being widely developed and CTO operational trials have also been conducted in Japan. This study develops means of estimating several important indices, including the compliance rate and mean expected delay, using data collected in the trial and shadow CTO operations. The estimation methods show variation in indices with differing maximum assigned CTO, while the analytical results suggest the optimal maximum assigned CTO. Furthermore, a variable maximum assigned CTO is proposed to improve the CTO operation. The analytical results show that the proposed method can improve the compliance rate as well as the mean expected delay.

INDEX TERMS Air traffic control, air traffic flow management (ATFM), traffic management initiatives (TMIs), calculated time over (CTO).

I. INTRODUCTION

A. BACKGROUND

Given limited air traffic control capacity, air traffic demand must not exceed airspace or airport capacity, including the processing capacity of air traffic controllers (ATCo) and the runway throughput. If traffic demand exceeds capacity, ATCo will instruct aircraft to delay their arrival using vectoring or airborne holding. However, since excessive vectoring and airborne holding increase aircraft fuel consumption, air traffic flow must be regulated in the event of excess demand. Accordingly, Air Traffic Flow Management (ATFM) is widely used to prevent the excess demand [1]. ATFM leverages various techniques to regulate air traffic flow, including ground delay/stop, minutes/miles-in-trail, speed adjustments and rerouting, which are collectively referred to as Traffic Management Initiatives (TMIs) [2].

In addition to the above TMIs, the Japan Civil Aviation Bureau has adopted a Calculated Fix Departure Time, also known as Calculated Time Over (CTO) [3]. The CTO is a TMI that assigns a time to fly over a specific waypoint for in-flight aircraft. Fig. 1 presents the procedure of the CTO operation. Here, ''CTO fix'' refers to the target waypoint where the aircraft has to fly over with the specified CTO. When the ATFM system predicts excess demand for an airspace or airport, it assigns a CTO to an aircraft. Within this figure, the time at which the ATFM system determines the CTO is 8:30, whereupon the ATCo instructs the pilot to cross the CTO fix at the assigned CTO. The original estimated time over (ETO) at the CTO fix is 9:28, while the CTO is assigned as 9:30. Accordingly, the aircraft must delay its ETO by 2 minutes. The pilot judges whether the aircraft can comply with the assigned CTO and replies by accepting or rejecting the CTO. The pilot also decides how to comply with the CTO, which usually involves varying the cruise speed. A similar concept, Long-Range ATFM, has been developed in New Zealand and Singapore [4]. The ground delay, which assigns the Expected Departure Clearance Time (EDCT) to departing aircraft, is also a time-assignment TMI, but is only assignable to flights departing from domestic airports. Accordingly, if only ground delay is used, only domestic flights will be delayed to prevent excess demand, resulting in an imbalance between domestic and inbound flights. In contrast, the CTO, assignable to both domestic and

The associate editor coordinating the review of this manuscript and approving it for publication was Rosario Pecora.

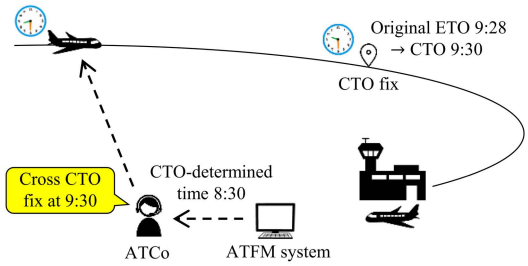

FIGURE 1. Procedure of CTO operation.

inbound flight, has the potential to improve the fairness of ATFM.

A trial operation of the CTO in Japan began in 2011 [5] but was suspended in 2014 due to the high rate of CTO rejection on the part of pilots. The data collected in the trial operation were analyzed to identify and resolve problems in the CTO operation. Additionally, for further data collection, a shadow operation, akin to "shadow testing" in software development, was conducted from 2020 to 2021, during which the CTO was not instructed to the pilot and the aircraft's cruise speed remained unchanged. Instead, fundamental CTO operation data were collected, such as ETO at a specific waypoint obtained from onboard and ground systems. By analyzing the data collected in the shadow operation, the operational procedure and ground systems will be improved and CTO trial operation will be resumed.

B. STATE OF THE ART

Having an in-flight speed control like the CTO allows the arrival time to be controlled without extra fuel consumption, while controlling the arrival time via vectoring or holding consumes more fuel than the speed control [6]–[9]. Previous studies have investigated the potential benefits of applying in-flight speed control to arrival management or ATFM. Jones *et al.* developed a speed control algorithm based on integer programming for transferring delay away from the terminal airspace to the en-route flight phase [10]. Moertl and Pollack also presented an airline-based sequencing and spacing system for arrival traffic, including a speed advisory function [12]–[14]. Several studies also proposed combining speed control in the en-route flight phase with a Ground Delay Program, which is a TMI to delay the departure time [12]–[14]. Andreeva-Mori *et al.* and Christien *et al.* combine the ATFM simulator, including the ground delay and CTO and terminal traffic simulator to examine how the enroute and terminal arrival traffic management interact [15], [16]. These studies performed simulations with realistic traffic scenarios to illustrate the potential benefits of in-flight speed control for ATFM. Additionally, Nancy *et al.* conducted a human-in-the-loop (HITL) simulation to demonstrate Integrated Demand Management (IDM) concept, which combines ATFM and Time-Based Flow Management, including in-flight speed control [17]. The results of the HITL simulation shows that the IDM can reduce excessive ground delay while ensuring fairness between domestic and inbound flights [18]. However, the above previous studies employed simple model for the CTO operation; for example, all the aircraft can make 2 minutes enroute delay. Matsuno and Andreeva-Mori developed a model-based approach to estimate the compliance rate of each flight [19]. They simulated the CTO flights based on Base of Aircraft Data provided by EUROCONTROL and calculated the key achievable delay parameter used to estimate the compliance rate. In contrast, the authors proposed a method of estimating the achievable delay and compliance rate by relying on analysis of data derived from the trial/shadow operations. In other words, the proposed approach can be considered a data-driven approach [20]. However, only the estimation method was proposed without any detailed analysis of the estimation results in Ref. [20]. Furthermore, the data collection period used to estimate the compliance rate equated to just half the shadow operation.

C. CONTRIBUTIONS

One important index in the CTO operation is the compliance rate, which expresses the level of assigned CTO with which a pilot can comply. A high CTO rejection rate disturbs air traffic and increases the workload for ATCos and pilots, which underlines the crucial need to develop a CTO procedure with a high compliance rate to deploy CTO operation successfully. This study aims to optimize CTO operation. To achieve the goal, the main contributions of this study are as follows:

- To estimate the compliance rate of the assigned CTO using data collected in trial and shadow operations.
- To analyze the estimation results to optimize CTO operational efficiency.
- To develop a means of improving the CTO operation, such as boosting the compliance rate and performance of the CTO operation.

The remainder of this paper is organized as follows. Section II describes the CTO operational model, including the operational environment and problem of the CTO operation, while Sections III and IV describe the trial and shadow operations, respectively. These sections also describe the data collected in each trial and the method used to analyze the collected data. Section V discusses the optimal CTO operation settings and proposes means of improvement, while Section VI provides the conclusion and outlines future work.

II. CTO OPERATIONAL MODEL

A. OPERATIONAL ENVIRONMENT OF CTO OPERATION

The applicability of the CTO is currently being considered for application to inbound arrival flights at Tokyo International Airport (RJTT), the busiest in Japan. Fig. 2 displays the four target routes to which to apply the CTO, which are referred to as Routes 1 to 4. The four routes enter Fukuoka Flight Information Region (Fukuoka FIR) from the west or southwest and enter the Tokyo Approach Control Area (Tokyo ACA) via the SPENS or SELNO waypoint to arrive at RJTT. Table 1 presents the CTO routes, CTO fix and the distance to the CTO fix respectively.

TABLE 1. CTO routes. Values in parentheses denote distances to the CTO fix in nautical miles.

Route	Waypoints	CTO fix	CTO-determined time
1	ONIKU–FUE–FLUTE–SPENS (537) (424) (0)	FLUTE	50 minutes before SPENS
2	MOLKA–MELEN–OTOWA–SELNO (738) (467) (0)	OTOWA	60 minutes before SELNO
3	BORDO/SEDKU/IGURU–TAMAK–YULIA–NUMKO–SELNO (822) (846) (861) (508) (108) (0)	NUMKO	60 minutes before SELNO
4	MEVIN/LEBIX–KAZIK/ALBAX–TAMAK–YULIA–NUMKO–SELNO (1047) (994) (879) (616) (508) (108) (0)	NUMKO	90 minutes before SELNO

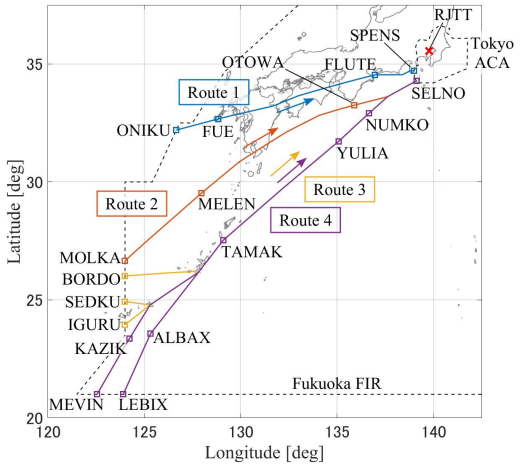

FIGURE 2. Target routes for CTO operation.

The CTO-determined time is defined as the remaining flight time to the entry waypoints to the Tokyo ACA such as SPENS and SELNO. The CTO-determined timings are when the aircraft flies over the vicinity of FUE, MELEN, TAMAK and KAZIK/ALBAX for each route. For example, the CTO in Route 2 is determined when the remaining flight time to SELNO is 60 minutes; then, the aircraft flies near MELEN. To maximize the ATFM capability, it may be useful to assign an earlier CTO than the original ETO, but only the delay is considered at this point.

B. PROBLEM OF CTO OPERATION

One obstacle to achieving a high compliance rate is that the ATFM system is unaware of whether the aircraft can comply with the assigned CTO when calculating it. The ATFM ground system can access various information related to the target aircraft when assigning the CTO, such as the route, aircraft type and cruise altitude and speed. However, the ATFM system cannot obtain the target aircraft's achievable delay. If this were possible, CTO rejection could be prevented by assigning a CTO within the achievable delay. The achievable delay is highly dependent on the minimum acceptable cruise speed. Note that the minimum acceptable cruise speed is not based only on the aircraft performance, such as the stall speed. During actual operation, the minimum cruise speed is determined by the pilot with various flight conditions taken into consideration, including the aircraft performance,

TABLE 2. Parameter definition for CTO operation.

Symbol	Name	Unit
Δt_{CTO}	Required delay by the assigned CTO	[min]
t_{det}	CTO-determined time	[-]
Δd_{achv}	Achievable delay	[min]
R_{cmp}	Compliance rate	[%]
$\Delta t_{CTO,max}$	Maximum Δt_{CTO} in the ATFM system	[min]

aircraft mass, wind conditions and safety margin. Accordingly, the minimum acceptable cruise speed differs for each flight. In addition, there are several parameters which the ATFM system cannot obtain, such as the Mach number deceleration rate. Therefore, the ATFM system cannot appropriately calculate the achievable delay.

C. SPEED PROFILE

One method to increase the compliance rate is to estimate the achievable delay, which can then be used to design the appropriate CTO operation. A CTO operation model is developed to do this, with relevant parameters defined in Table 2 and Fig. 3. Each aircraft is assigned Δt_{CTO} calculated by the ATFM system at t_{det}. The ATFM algorithm for the EDCT/CTO assignment was shown in Ref. [21]. In addition, Δd_{achv} is inherent in each aircraft depending on the flight conditions. Subsequently, if Δt_{CTO} is below Δd_{achv}, the pilot accepts the assigned CTO. In the case presented in Fig. 3, three out of four aircraft comply with the assigned CTO; accordingly, R_{cmp} is 75 %. $\Delta t_{CTO,max}$ is an ATFM algorithm parameter and Δt_{CTO} is assigned within $\Delta t_{CTO,max}$. At present, $\Delta t_{CTO,max}$ is considered constant for each route in the ATFM system, which is why all aircraft in Fig. 3 are assigned Δt_{CTO} within $\Delta t_{CTO,max}$. Although it is desirable to increase $\Delta t_{CTO,max}$ to boost the ATFM algorithm performance, doing so could cause R_{cmp} to decline. Accordingly, $\Delta t_{CTO,max}$ must be set appropriately to achieve a high R_{cmp}. The CTO is determined at t_{det}. An earlier t_{det} can produce a larger Δd_{achv}, but an earlier t_{det} may result in a trajectory prediction error. Accordingly, t_{det} must also be set appropriately, although any impact of trajectory prediction error is outside the scope of this study.

Fig. 4 presents the CTO operational model, with CTO operational steps as follows:

(1) The aircraft cruises at m_1.
(2) The ATFM system determines t_{CTO} at t_{det}.

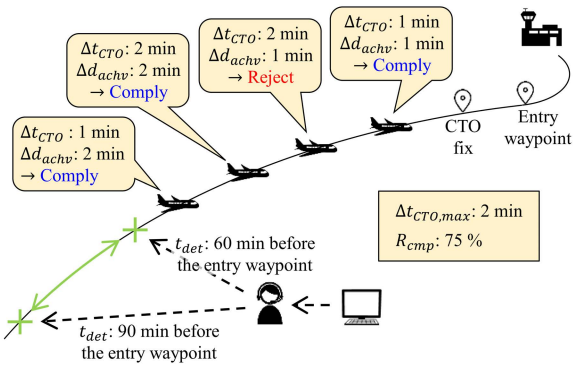

FIGURE 3. Parameter definition for CTO operation.

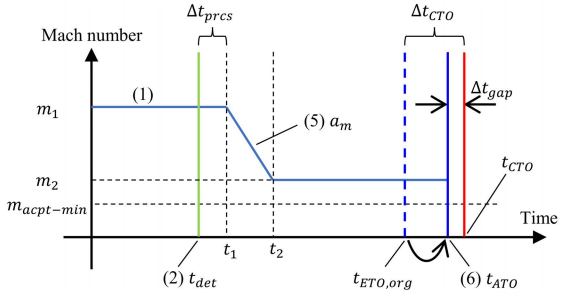

FIGURE 4. CTO operational model.

(3) The ATCo instructs the CTO to the pilot.
(4) The pilot judges whether the CTO is acceptable and controls the aircraft to comply with t_{CTO}.
(5) The aircraft decelerates with a_m to and cruises at m_2.
(6) The aircraft flies over the CTO fix at t_{ATO}.

Here, t_{CTO} is the assigned CTO. Then, Δt_{CTO} can be derived by $t_{CTO} - t_{ETO,org}$, where $t_{ETO,org}$ is the original ETO. m_1 and m_2 are the original cruise and decelerated Mach numbers, respectively. a_m is the deceleration rate of the Mach number. t_1 and t_2 are the start and end times of the deceleration, respectively. t_{ATO} is the actual time over at the CTO fix. Δt_{gap} is the gap between t_{CTO} and t_{ATO}. After the CTO is assigned, the aircraft starts decelerating to comply therewith. There is a delay from the CTO-determined time to the start of deceleration due to the processing time by the ATCo and pilot, e.g. during voice communication. The delay by the processing time is defined as Δt_{prcs}. By the deceleration, the time of arrival at the CTO fix is delayed. The gap Δt_{gap} is defined as $t_{ATO} - t_{CTO}$; accordingly, when Δt_{gap} is positive, the aircraft flies over the CTO fix later than t_{CTO} and vice versa. It is difficult for the aircraft to fly over the CTO fix at the exact t_{CTO}. Accordingly, if Δt_{gap} is sufficiently small, it is assumed that the aircraft can comply with the assigned CTO; even though the compliance threshold remains under discussion. $m_{acpt-min}$ denotes the acceptable minimum cruise Mach number. Δd_{achv} is maximized when m_2 is equal to $m_{acpt-min}$. If Δd_{achv} is smaller than Δt_{CTO} even with $m_{acpt-min}$, the pilot is liable to reject the assigned CTO.

Here, if Δt_{prcs}, a_m, and $m_{acpt-min}$ can be derived, Δd_{achv} can be calculated based on the model, as illustrated in Fig. 4. However, since the ATFM system cannot directly derive these three parameters, further modeling or data collection is required to calculate Δd_{achv}. Accordingly, these parameters are estimated or derived from the data collected in the trial/shadow operations.

III. TRIAL OPERATION FROM 2011 TO 2014

A. COLLECTED DATA IN TRIAL OPERATION

The CTO trial operation was conducted from 2011 to 2014. During this period, although the routes and airspace configuration differed from those in Fig. 2, the actual data for performing the CTO operation were available, including output data from the ATFM system and radar data. The data from ATFM system included t_{det}, t_{CTO}, CTO fix, callsign, and aircraft type of the target aircraft for the CTO operation. The radar data comprised the time, latitude, longitude, and pressure altitude. Although the radar data did not contain the Mach number, it could be estimated by synthesizing the time derivative of the position and wind data. Details of the Mach number estimation are shown in Appendix A. Figs. 5 and 6 present example results for cases in which the aircraft could and could not comply with the assigned CTO, respectively. Here, it was assumed that the aircraft could comply with the assigned CTO if Δt_{gap} was within ± 0.5 minutes. The horizontal axis of the pressure altitude/Mach number is Japan Standard Time (JST). The Mach number oscillates because it is estimated from the radar data and includes estimation noise. In both cases, the aircraft was assigned a later CTO than the original ETO at the CTO fix, whereupon the aircraft reduced Mach number accordingly. In Fig. 5, the aircraft could comply with the assigned CTO because Δt_{gap} was within ± 0.5 minutes. In contrast, Δt_{gap} in Fig. 6 was outside ± 0.5 minutes and negative. This result demonstrates that the aircraft flew over the CTO fix earlier than the assigned CTO and was unable to comply with the assigned CTO. Presumably, the achievable delay was smaller than that required, even if the aircraft decelerated to the acceptable minimum Mach number. If the CTO could be assigned appropriately considering Δd_{achv}, the aircraft might even be able to comply with the CTO in this case.

B. OPTIMIZATION-BASED MACH NUMBER ESTIMATION

During the trial operation from 2011 to 2014, the CTO was actually instructed from the ATCo to the pilot and the aircraft altered its speed to comply with the assigned CTO. Accordingly, Δt_{prcs} and a_m parameters described in II-C could be collected from the trial operation results. However, the Mach number profile included estimation noise as shown in Figs. 5 and 6. To estimate a clean Mach number profile, as illustrated in Fig. 4, optimization-based Mach number estimation was performed. The Mach number estimation problem can be formulated as follows:

$$\boldsymbol{x} = [t_1 \;\; t_2 \;\; m_1 \;\; m_2]^T, \tag{1}$$

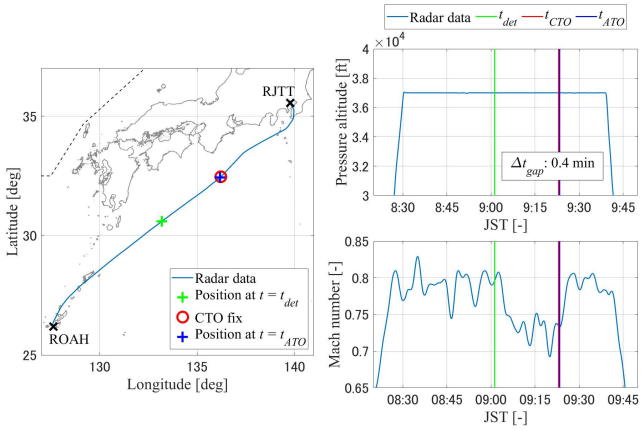

FIGURE 5. Example from the trial operation in the case that the aircraft could comply with the assigned CTO.

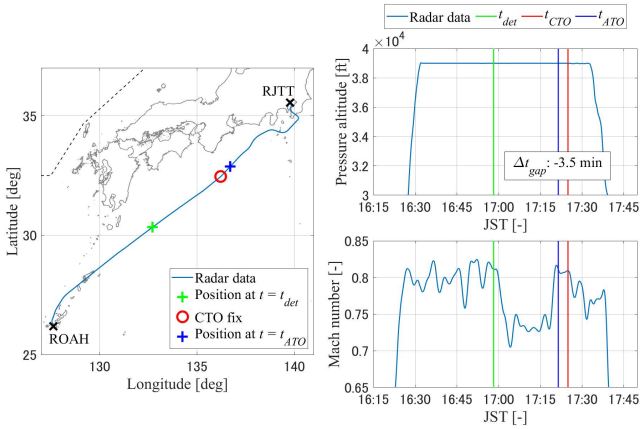

FIGURE 6. Example from the trial operation in the case that the aircraft could not comply with the assigned CTO.

$$\min_{x} \begin{cases} (m(t) - m_1)^2 & \text{if } t_0 \le t < t_1 \\ (m(t) - (a_m(t - t_1) + m_1))^2 & \text{if } t_1 \le t < t_2 \\ (m(t) - m_2)^2 & \text{otherwise,} \end{cases} \tag{2}$$

$$\begin{aligned} t_{det} &\le t_1, \\ t_1 &\le t_2, \\ t_2 &\le t_f, \end{aligned} \tag{3}$$

where t_{det}, t_1, t_2, m_1, and m_2 correspond to the parameters in Fig. 4. $m(t)$ is the Mach number including the estimation noise. t_0 and t_f are the initial and terminal time of $m(t)$, respectively. In this case, t_0 was set as the entry time to the Fukuoka FIR or the time at the top of climb and t_f was set as t_{ATO}. In addition, a_m can be derived as follows:

$$a_m = \frac{m_2 - m_1}{t_2 - t_1}. \tag{4}$$

The formulated optimization problem is a type of non-linear programming problem and solvable using a general purpose nonlinear programming solver. We used the MATLAB® fmincon function to solve this problem.

Fig. 7 and Table 3 present the optimization results of the flight shown in Fig. 5. The optimization results can estimate

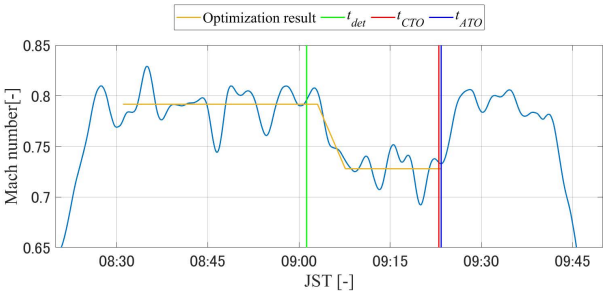

FIGURE 7. Example results of optimization-based Mach number estimation.

TABLE 3. Example results of optimization-based Mach number estimation.

Parameters	Value	Unit
m_1	0.79	[-]
m_2	0.73	[-]
Δt_{prcs}	1.8	[min]
a_m	-0.014	[1/min]

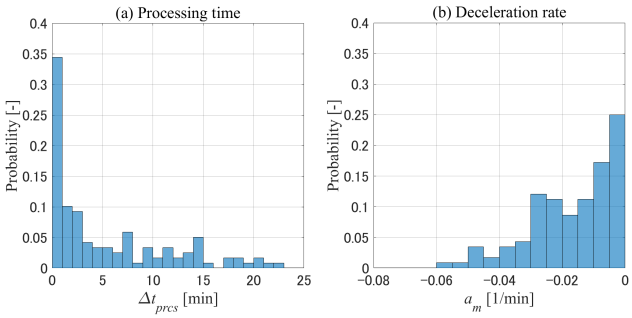

FIGURE 8. Distribution of the (a) processing time by the ATCo and pilot and the (b) deceleration rate of the Mach number.

TABLE 4. Average and median processing time by the ATCo and pilot (Δt_{prcs}) and the deceleration rate of the Mach number (a_m).

Parameters	Average	Median	Unit
Δt_{prcs}	5.4	2.4	[min]
a_m	-0.017	-0.013	[1/min]

a clean Mach number from the Mach number derived by the radar data. The optimization-based Mach number estimation is performed for all available data, including 153 flights. Fig. 8 presents the distribution of Δt_{prcs} and a_m. Note that not all the flights delayed their arrival as much as possible in the actual operation. Several flights could comply with the assigned CTO without deceleration. As a result, several flights had an excessive Δt_{prcs}. Table 4 presents the average and median of Δt_{prcs} and a_m. Due to the flights without deceleration, the average Δt_{prcs} is more than twice the median Δt_{prcs}. The purpose of this analysis is to extract the representative value of Δt_{prcs} and a_m under circumstances where the aircraft delayed their arrival as much as possible. Accordingly, the median value of Δt_{prcs} and a_m is used to reduce the effect from the excessive values.

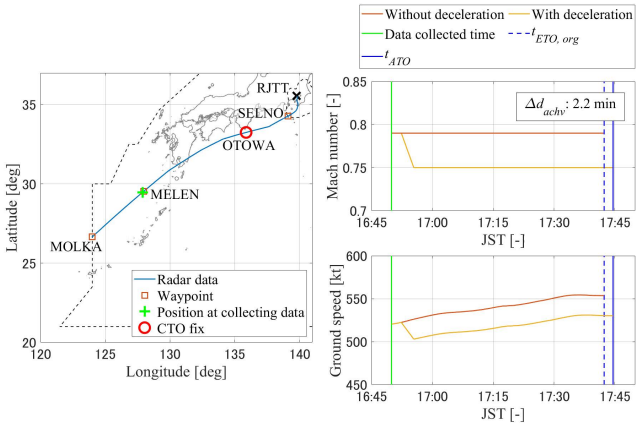

FIGURE 9. Example results of the achievable delay estimation.

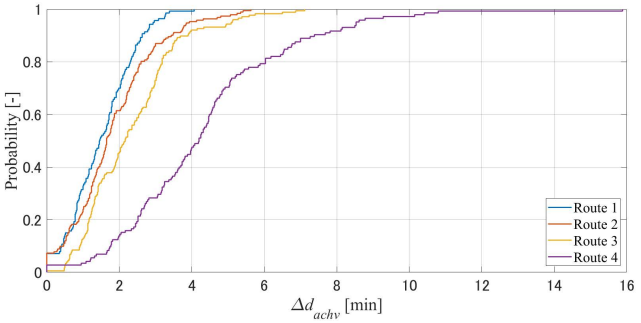

FIGURE 10. CDF of the achievable delay in each route.

IV. SHADOW OPERATION

A. COLLECTED DATA IN SHADOW OPERATION

The shadow operation was conducted from September to December 2020 and June to July 2021. During the shadow operation, although the aircraft did not actually decelerate, several data related to the CTO operation were collected from the onboard system via voice communication. The data collected included the CTO fix, the time at which the ATCo requested the onboard data from the pilot, cruise altitude, cruise Mach number, acceptable maximum/minimum Mach number and the callsign and target aircraft type. The collected data were combined with the corresponding radar data to obtain a time history of position and altitude. The available data included a total of 654 flights, namely 140 in Route 1, 192 in Route 2, 177 in Route 3 and 145 in Route 4 respectively. As mentioned in II-C, the achievable delay Δd_{achv} can be calculated if Δt_{prcs}, a_m, and $m_{acpt-min}$ are available. The collected data included $m_{acpt-min}$. Therefore, Δd_{achv} could be estimated by applying Δt_{prcs} and a_m derived in III-B to the shadow operation data. Furthermore, the compliance rate in the shadow operation could be estimated using the estimated Δd_{achv}.

B. SIMULATION-BASED COMPLIANCE RATE ESTIMATION

A numerical simulation is used to estimate Δd_{achv}, during which the flight trajectory is calculated based on integral calculation with the following assumptions:

- The aircraft flew along CTO routes.
- The aircraft remained at cruise altitude, with the cruise Mach number as collected data from the shadow operation.
- The time at which the ATCo collected the data was considered the CTO-determined time t_{det}.

Accordingly, the time history of the Mach number is set based on the CTO operational model as follows:

(1) Add Δt_{prcs} to t_{det} to derive the time to start deceleration.
(2) Decelerate by a_m to $m_{acpt-min}$.
(3) Cruise at $m_{acpt-min}$ until reaching the CTO fix.

Details of the trajectory simulation are shown in Appendix B.

Fig. 9 presents an example result of the simulation. In this example, the aircraft flew along Route 2, the CTO fix of which was OTOWA waypoint. The data were collected around MELEN and $m_{acpt-min}$ was 0.75. On the right side of Fig. 9, the Mach number is plotted from the time of data collection, which is assumed as t_{det}. Here, "Without deceleration" denotes the case in which the aircraft remains at the cruise Mach number to derive the original ETO, while "With deceleration" denotes the case in which the aircraft decelerates to $m_{acpt-min}$ to delay its arrival as much as possible. After Δt_{prcs}, the aircraft decelerates by a_m to $m_{acpt-min}$. Note that the ground speed changes affected the wind effects, despite the fact the aircraft cruises at a constant Mach number. In the case without deceleration, $t_{ETO,org}$ is 17:42:20, while t_{ATO} with deceleration was 17:44:31. As a result, Δd_{achv} can be estimated as 2.2 minutes in this flight.

Fig. 10 presents the simulation results for all the flights. Each cumulative distribution function (CDF) denotes Δd_{achv} in each route. Fig 10 also presents the compliance rate R_{cmp} for the maximum assigned CTO $\Delta t_{CTO,max}$. For example, Route 1 is 0.7 at 2 minutes, signifying that the remaining 30 % of flights can comply with a delay of two minutes or more; namely, R_{cmp} is equal to 30 % in Route 1 when $\Delta t_{CTO,max}$ is equal to 2. Table 5 shows R_{cmp} in each route with different $\Delta t_{CTO,max}$. The results show that a longer route distance provides higher R_{cmp}. Route 4 is the longest, followed in order by Routes 3, 2 and 1. Additionally, over all routes, a shorter $\Delta t_{CTO,max}$ provides higher R_{cmp}.

V. DISCUSSION

A. OPTIMAL PARAMETER FOR ATFM SYSTEM

Δd_{achv} and R_{cmp} could be estimated by combining optimization-based Mach number estimation and simulation-based compliance rate estimation. The results showed that shorter $\Delta t_{CTO,max}$ can lead higher R_{cmp}. Here, high R_{cmp} is important to deploy the CTO operation successfully, as mentioned in I-C. However, the shortest $\Delta t_{CTO,max}$ or all routes are not appropriate, because setting long $\Delta t_{CTO,max}$ is desirable with the performance of the CTO operation in the ATFM in mind. $\Delta t_{CTO,max}$ and R_{cmp} have a trade-off relationship. Accordingly, there is a question how to set the longest $\Delta t_{CTO,max}$ while the reduction of R_{cmp} remains within a reasonable range. One of the important perspectives

TABLE 5. CTO compliance rate in percentage for each route with different maximum assigned CTO.

$\Delta t_{CTO,max}$	1 [min]	2 [min]	3 [min]	4 [min]	5 [min]
Route 1	68.6	30.0	4.3	0.7	0.0
Route 2	77.1	38.5	14.1	4.7	2.6
Route 3	87.6	54.8	27.1	7.9	5.6
Route 4	96.6	86.2	71.7	53.1	29.7

for the ATFM is the extent of delay assignable to in-flight aircraft using the CTO operation. As mentioned in I-A, this operation has the potential to improve fairness between domestic and inbound flights by transferring ground delay to in-flight delay. Accordingly, $\Delta t_{CTO,max}$ maximizing the expected delay performed by the CTO is optimal setting in terms of the ATFM. Here, the mean expected delay performed by the CTO operation $\widehat{\Delta d}_{CTO,mean}$ can be derived as follows:

$$\widehat{\Delta d}_{CTO,mean} = \Delta t_{CTO,max} \frac{R_{cmp}}{100}. \tag{5}$$

$\widehat{\Delta d}_{CTO,mean}$ is the expected delay per flight if a specified $\Delta t_{CTO,max}$ is applied. Table 6 shows $\widehat{\Delta d}_{CTO,mean}$ with different $\Delta t_{CTO,max}$ in each route. The results indicate that the optimal $\Delta t_{CTO,max}$ are 1, 1 or 2 or 2 and 3 minutes in Routes 1 to 4 denoted by the red values.

Note that the optimal $\Delta t_{CTO,max}$ in Table 6 is just maximizing $\widehat{\Delta d}_{CTO,mean}$ in each route. However, the corresponding R_{cmp} is not necessarily acceptable for CTO operation, particularly for ATCo and pilots. For example, the optimal $\Delta t_{CTO,max}$ in Route 3 is two minutes, but the corresponding R_{cmp} is just equal to 54.8 % as shown in Table 5. In this case, it is highly probable that 45.2 % of flights reject the assigned CTO and a rejection rate as high as this might be unacceptable for ATCo and pilots from a workload perspective.

B. IMPROVEMENT METHOD FOR CTO OPERATION

To resolve the high rejection rate, we propose variable $\Delta t_{CTO,max}$. Depending on the flight conditions, each flight possesses different Δd_{achv}, so R_{cmp} can be increased if the ATFM system can apply small $\Delta t_{CTO,max}$ to a flight with small Δd_{achv}. Furthermore, such a variable $\Delta t_{CTO,max}$ might also increase $\widehat{\Delta d}_{CTO,mean}$. The length of Δd_{achv} is highly dependent on the difference between m_1 and $m_{acpt-min}$. Fig. 11 shows the correlation between Δm and Δd_{achv} in each route. Δm is the difference between m_1 and $m_{acpt-min}$, and R_{corr} is the correlation coefficient between Δm and Δd_{achv}. If the Δm of each flight can be derived, the ATFM system can change $\Delta t_{CTO,max}$ depending on Δm. However, the ATFM system cannot derive $m_{acpt-min}$ in actual operation, while m_1 can be estimated. Therefore, we consider to vary $\Delta t_{CTO,max}$ only depending on m_1 as shown in Fig. 12. A flight with high cruise Mach number is assigned large $\Delta t_{CTO,max}$ and vise versa, because Δm tends to be larger with larger m_1. Here, $m_{crz,th}$ is the threshold for m_1 in the variable $\Delta t_{CTO,max}$. In this case, $\Delta t_{CTO,max}$ is set as 2 minutes, but one minute of $\Delta t_{CTO,max}$ is applied to a flight with m_1 below $m_{crz,th}$,

TABLE 6. Mean expected delay performed by the CTO operation in minutes for each route with different maximum assigned CTO. The red values are the maximum mean expected delay in each route.

$\Delta t_{CTO,max}$	1 [min]	2 [min]	3 [min]	4 [min]	5 [min]
Route 1	0.686	0.600	0.129	0.029	0.00
Route 2	0.771	0.771	0.422	0.188	0.130
Route 3	0.876	1.096	0.814	0.316	0.282
Route 4	0.966	1.724	2.152	2.124	1.483

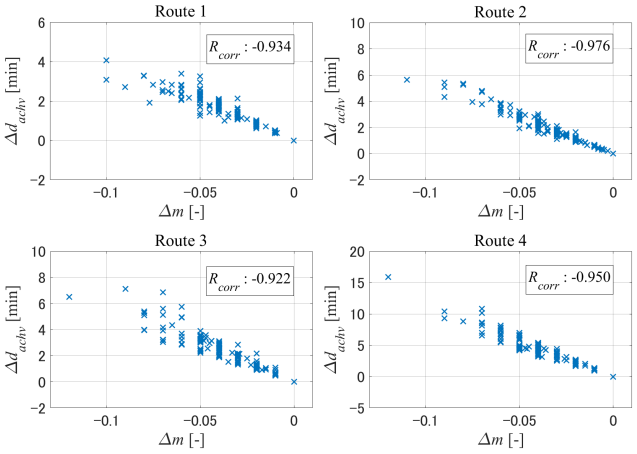

FIGURE 11. Correlation between the difference of Mach number and achievable delay.

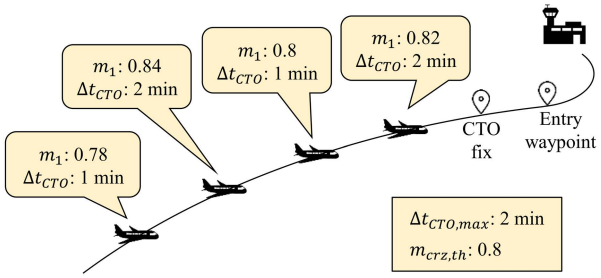

FIGURE 12. Improvement method for the CTO operation.

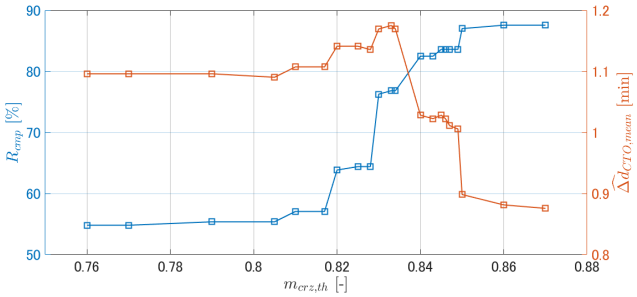

FIGURE 13. Variation of the compliance rate and mean expected delay with different cruise Mach number threshold.

Fig. 13 shows the variation of R_{cmp} and $\widehat{\Delta d}_{CTO,mean}$ with different $m_{crz,th}$ in Route 3. In Route 3, the minimum m_1 was 0.77 and the maximum m_1 was 0.87. Accordingly,

$m_{crz,th} = 0.76$ corresponds to two minutes of $\Delta t_{CTO,max}$ are applied to all flights; hence, R_{cmp} and $\widehat{\Delta d}_{CTO,mean}$ at $m_{crz,th} = 0.76$ are equal to the results of Tables 5 and 6 in Route 3 with 2 minutes of $\Delta t_{CTO,max}$. Similarly, $m_{crz,th} = 0.87$ corresponds to one minute of $\Delta t_{CTO,max}$ being applied to all flights. In Fig. 13, by increasing $m_{crz,th}$, the number of flights to which one minute of $\Delta t_{CTO,max}$ is applied increases, whereupon R_{cmp} and $\widehat{\Delta d}_{CTO,mean}$ also increase due to the decline in CTO rejections. However, too high $m_{crz,th}$ decreases $\widehat{\Delta d}_{CTO,mean}$, because a few flights are applied 2 minutes of $\Delta t_{CTO,max}$ with high $m_{crz,th}$. Consequently, R_{cmp} increases with higher $m_{crz,th}$, while $\widehat{\Delta d}_{CTO,mean}$ is convex upward. Fig. 13 shows that 0.833 of $m_{crz,th}$ maximizes $\widehat{\Delta d}_{CTO,mean}$; then, R_{cmp} is equal to 76.8 %. If an acceptance rate of 76.8 % is acceptable for ATCo and pilots, the variable $\Delta t_{CTO,max}$ with 0.833 of $m_{crz,th}$ is the optimal settings for the CTO operation in Route 3. Furthermore, the corresponding $\widehat{\Delta d}_{CTO,mean}$, 1.175 minutes, exceeds any $\widehat{\Delta d}_{CTO,mean}$ without variable $\Delta t_{CTO,max}$ in Route 3 shown in Table 6.

VI. CONCLUSION

This paper analyzed the CTO operation to improve the compliance rate and performance. The optimization-based Mach number estimation and simulation-based compliance rate estimation were developed to estimate the achievable delay and compliance rate from the data collected during the trial and shadow operations. The analysis results showed that there is a trade-off relationship between the maximum assigned CTO and compliance rate. The optimal configuration of the maximum assigned CTO was also discussed to maximize the mean expected delay performed by the CTO. Furthermore, the variable maximum assigned CTO was also proposed to improve the compliance rate and mean expected delay. Applying the proposed method, boosted the compliance rate by 22.0 % and the expected delay also increased by 0.079 minutes per flight.

Future work will address work to evaluate the CTO operation in the air traffic. The compliance rate and mean expected delay obtained in this paper can underpin the CTO operation. By introducing the model to the ATFM simulator, as shown in Refs. [15], [21], the ATFM simulator can simulate air traffic more realistically with CTO operation. Consequently, the simulation will be capable of evaluating the potential benefits of CTO operation. In addition, such a realistic simulation can investigate the interaction between ATFM and ATCo's separation management. If an aircraft rejects the assigned CTO, it may have conflict with other aircraft complying with the assigned CTO in the same route. Future work will also address the effects of the different CTO operational configuration to the overall air traffic.

APPENDIX A
MACH NUMBER ESTIMATION

The Mach number is estimated from the radar and wind data via the following steps:

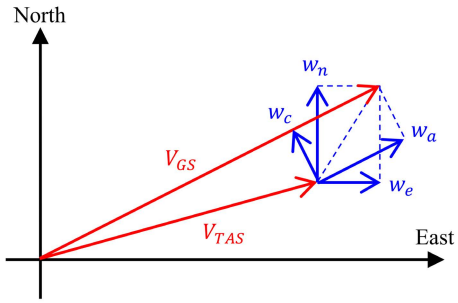

FIGURE 14. Geometry of GS, TAS, and wind speed.

- The geodetic length and azimuth angle of the trajectory are calculated from latitude and longitude using inverse calculation [22].
- The ground speed (GS) is derived from the time derivative of the geodetic length.
- The true airspeed (TAS) is estimated by synthesizing the GS with wind data according to Eq. (6).

$$V_{TAS} = \sqrt{(V_{GS} - w_a)^2 + w_c^2}. \tag{6}$$

V_{TAS} is the TAS, V_{GS} is the GS, w_a is the along-track wind speed and w_c is the cross-track wind speed, respectively. The geometry of the GS, TAS and wind speed are shown in Fig. 14, where w_n and w_e are the meridional and zonal winds. The wind data is derived from the numerical weather prediction (NWP) data based on the meso-scale model (MSM) provided by the Japan Meteorological Agency [23].

- m is calculated from V_{TAS} by using Eq. (7).

$$m = \frac{V_{TAS}}{\sqrt{\kappa RT}}, \tag{7}$$

where κ is the heat capacity ratio for air and R is the real gas constant for air. T is the atmospheric temperature which also obtainable from NWP MSM data.

APPENDIX B
TRAJECTORY SIMULATION

A flowchart of the trajectory simulation is shown in Fig. 15, the initial position of which is $t = t_{det}$. The trajectory is calculated by the time integral of V_{GS} from the initial position to the CTO fix, while m is generated from the time history of the Mach number described in IV-B and converted to V_{TAS} according V to Eq. (8).

$$V_{TAS} = m\sqrt{\kappa RT}. \tag{8}$$

V_{GS} is calculated by synthesizing V_{TAS} and NWP MSM wind data, as follows:

$$V_{GS} = \sqrt{V_{TAS}^2 - w_c^2} + w_a. \tag{9}$$

The trajectory simulation is terminated when the aircraft reaches the CTO fix. Then, t_{ATO} can be obtained.

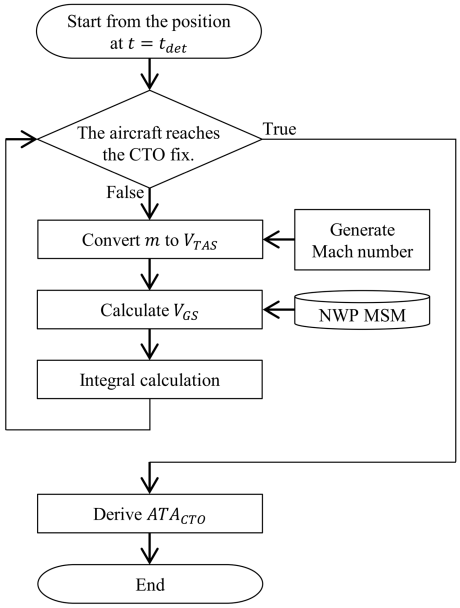

FIGURE 15. Flowchart of the trajectory simulation.

ACKNOWLEDGMENT

The authors would like to thank the Japan Civil Aviation Bureau for providing the radar, ATFM, and shadow operation data.

REFERENCES

[1] T. Ishikawa, "Sharing of experience from implementing the Japan ATFM and CDM meeting at ATM center," presented at the ATFM Workshop Asia Pacific, 2014. [Online]. Available: https://www.icao.int/APAC/APAC-RSO/Pages/Presentations.aspx

[2] Federal Aviation Administration, Air Traffic Plans and Publications. *Traffic Management Initiatives*. Accessed: Jul. 2022. [Online]. Available: https://www.faa.gov/air_traffic/publications/atpubs/foa_html/chap18_section_7.html

[3] Japan Civil Aviation Bureau, "ATFM/CDM in Japan," presented at the 3rd Meeting Air Traffic Flow Manage. Steering Group, 2014. [Online]. Available: https://www.icao.int/APAC/Meetings/Pages/2014-ATFM-SG3.aspx

[4] New Zealand and Singapore, "Long range ATFM concept trials," in *Proc. 8th Meeting Asia/Pacific Air Traffic Flow Manage. Steering Group (ATFM/SG)*, 2018, pp. 1–9.

[5] *Operational Trial for Specifying Calculated Fix Departure Time (SCAS) for Air Traffic Flow Management*, Japan Civil Aviation Bureau, Japan Aeronautical Information Service Center, Aeronautical Information Circular, Tokyo, Japan, Jul. 2011. [Online]. Available: https://en.wikipedia.org/wiki/Aeronautical_Information_Publication

[6] X. Prats and M. Hansen, "Green delay programs, absorbing ATFM delay by flying at minimum fuel speed," in *Proc. 9th USA/Eur. Air Traffic Manage. Res. Develop. Seminar (ATM Seminar)*, Berlin, 2011, pp. 1–8.

[7] Y. Xu, R. Dalmau, and X. Prats, "Effects of speed reduction in climb, cruise and descent phases to generate linear holding at no extra fuel cost," in *Proc. 7th Int. Conf. Res. Air Transp. (ICRAT)*, Philadelphia, 2016. [Online]. Available: https://www.icrat.org/previous-conferences/7th-international-conference/ICRAT%202016%20Final%20v3.pdf and https://drive.google.com/file/d/1eTxh_DR3vKTTbjttKZAIwE0kVfWU-yi3/view

[8] Y. Xu, R. Dalmau, and X. Prats, "Maximizing airborne delay at no extra fuel cost by means of linear holding," *Transp. Res. C, Emerg. Technol.*, vol. 81, pp. 137–152, Aug. 2017.

[9] Y. Xu and X. Prats, "Linear holding for airspace flow programs: A case study on delay absorption and recovery," *IEEE Trans. Intell. Transp. Syst.*, vol. 20, no. 3, pp. 1042–1051, Mar. 2019.

[10] J. C. Jones, D. J. Lovell, and M. O. Ball, "En route speed control methods for transferring terminal delay," in *Proc. 10th USA/Eur. Air Traffic Manage. Res. Develop. Seminar (ATM Seminar)*, Chicago, 2013, Paper 325. [Online]. Available: https://www.atmseminar.org/10th-seminar/papers/

[11] P. M. Moertl and M. E. Pollack, "Airline based en route sequencing and spacing field test results, observations and lessons learned for interval management," in *Proc. 9th USA/Eur. Air Traffic Manage. Res. Develop. Seminar (ATM Seminar)*, Berlin, 2011, pp. 1–10.

[12] L. Delgado and X. Prats, "Effect of radii of exemption on ground delay programs with operating cost based cruise speed reduction, case study: Chicago O'Hare international airport," in *Proc. 10th USA/Eur. Air Traffic Manage. Res. Develop. Seminar (ATM Seminar)*, Chicago, 2013, Paper 270. [Online]. Available: https://www.atmseminar.org/10th-seminar/papers/

[13] J. C. Jones, D. J. Lovell, and M. O. Ball, "Combining control by CTA and dynamic enroute speed adjustment to improve ground delay program performance," in *Proc. 11th USA/Eur. Air Traffic Manage. Res. Develop. Seminar (ATM Seminar)*, Lisbon, 2015, pp. 1–47.

[14] Y. Xu and X. Prats, "Including linear holding in air traffic flow management for flexible delay handling," in *Proc. 12th USA/Eur. Air Traffic Manage. Res. Develop. Seminar (ATM Seminar)*, Seattle, 2017, Paper 139. [Online]. Available: https://www.atmseminar.org/12th-seminar/papers/

[15] A. Andreeva-Mori, D. Toratani, M. Onji, and Y. Matsuno, "Quantitative evaluation of controlled arrival flow connecting into point merge system at Tokyo international airport," in *Proc. Asia–Pacific Int. Symp. Aerosp. Technol. (APISAT)*, 2021. [Online]. Available: https://link.springer.com/book/9789811926884

[16] R. Christien, E. Hoffman, and K. Zeghal, "En-route traffic overflows versus arrival management delays," *J. Air Transp.*, vol. 28, no. 4, pp. 164–172, Oct. 2020.

[17] N. M. Smith, C. Brasil, P. U. Lee, N. Buckley, C. Gabriel, C. P. Mohlenbrink, F. Omar, B. Parke, C. Speridakos, and H.-S. Yoo, "Integrated demand management: Coordinating strategic and tactical flow scheduling operations," in *Proc. 16th AIAA Aviation Technol., Integr., Oper. Conf.*, Washington, DC, USA, Jun. 2016, Paper AIAA 2016-4221. [Online]. Available: https://arc.aiaa.org/doi/10.2514/6.2016-4221

[18] H.-S. Yoo, C. Brasil, N. M. Smith, P. U. Lee, C. P. Mohlenbrink, N. Buckley, A. Globus, and G. Hodell, "Integrated demand management: Minimizing unanticipated excessive departure delay while ensuring fairness from a traffic management initiative," in Proc. 17th AIAA Aviation Technol., Integr., Operations Con., Denver, CO, USA, 2017, Paper AIAA 2017-4100. [Online]. Available: https://arc.aiaa.org/doi/abs/10.2514/6.2017-4100

[19] Y. Matsuno and A. Andreeva-Mori, "Analysis of achievable airborne delay and compliance rate by speed control: A case study of international arrivals at Tokyo international airport," *IEEE Access*, vol. 8, pp. 90686–90697, 2020.

[20] D. Toratani, Y. Nakamura, and M. Oka, "Data-driven analysis method for calculated time over in air traffic flow management," in *Proc. 14th USA/Eur. Air Traffic Manage. Res. Develop. Seminar (ATM Seminar)*, 2021, Paper 46. [Online]. Available: https://www.atmseminar.org/upcoming-seminar/papers-and-presentations/

[21] D. Toratani, N. Takeichi, and M. Oka, "Simulation study on the interoperability between air traffic flow management and tactical arrival management," in *Proc. ENRI Int. Workshop ATM/CNS (EIWAC)*, Tokyo, 2019, Paper EN-A-91. [Online]. Available: https://www.enri.go.jp/eiwac/eiwac_2019_eng.html

[22] B. R. Bowring, "Total inverse solutions for the geodesic and great elliptic," *Surv. Rev.*, vol. 33, no. 261, pp. 461–476, Jul. 1996.

[23] Japan Meteorological Agency. *JMA Numerical Weather Prediction*. Accessed: May 2022. [Online]. Available: https://www.jma.go.jp/jma/jma-eng/jma-center/nwp/nwp-top.htm

DAICHI TORATANI received the B.Eng., M.Eng., and Ph.D. degrees from Yokohama National University, in 2011, 2012, and 2016, respectively. Since 2016, he has been with the Electronic Navigation Research Institute and the National Institute of Maritime, Port and Aviation Technology. His research interests include air traffic management and unmanned aircraft systems, particularly optimization, simulation, and system design applications.

YOICHI NAKAMURA received the M.E. and Ph.D. degrees in aerospace engineering from Nagoya University, in 2012 and 2015, respectively. He joined ENRI, in 2012, before receiving his Ph.D. degree. He is currently an ATM Researcher at the Electronic Navigation Research Institute. His research interests include ATM performance assessment and aviation weather.

MEGUMI OKA received the B.Eng. degree from Yamaguchi University, in 1996. She has been with the Electronic Navigation Research Institute, since 1996. Her research interests include air traffic management and data science.